Viscous potential flow analysis of capillary instability with heat and mass transfer

Hyungjun Kim* and Sejin Kwon†
Department of Aerospace Engineering, KAIST, Daejeon, 305-701, South Korea

Juan C. Padrino
Dept. Aerospace Engineering and Mechanics, University of Minnesota, Minneapolis, MN 55455, USA

Toshio Funada
Dept. Digital Engineering, Numazu College of Technology, Ooka 3600, Numazu, Shizuoka 410-8501, Japan
(Dated: October 12, 2007)

We carry out the linear viscous-irrotational analysis of capillary instability with heat transfer and phase change. We consider the cylindrical interface shared by two viscous incompressible fluids enclosed by two concentric cylinders. In viscous potential flow, viscosity enters the model through the balance of normal stresses at the interface. We write the dispersion relation from the stability analysis for axisymmetric disturbances in terms of a set of dimensionless numbers that arise in this phase change problem. For the film boiling condition, plots depicting the effect of some of these parameters on the maximum growth rate for unstable perturbations and critical wavenumber for marginal stability are presented and interpreted. Viscous effects of a purely irrotational motion in the presence of heat and mass transfer can stabilize an otherwise unstable gas-liquid interface.

I. INTRODUCTION

The problem of Rayleigh-Taylor and Kelvin-Helmholtz instability with heat and mass transfer across the liquid-vapor interface was formulated for potential flow of an inviscid fluid by Hsieh [1, 2]. He modeled 'small' perturbations of a plane interface between two fluids bounded by two parallel plates. Hsieh [2] found that when the vapor layer is hotter than the liquid layer, the presence of heat and mass transfer mitigates, but does not suppresses, the growth of unstable perturbations; however, the classical stability criterion remains unaltered. Regarding Kelvin-Helmholtz instability, the classical stability criterion is modified when heat and mass transfer are included in the analysis, although the heat flux does not appear in the relation. Nayak and Chakraborty [3] studied the Kelvin-Helmholtz stability of the cylindrical interface between the liquid and vapor phases with heat and mass transfer. Lee [4, 5] studied Rayleigh and Kelvin-Helmholtz instabilities in phase change problems with mass transfer for the fluid motion in a cylindrical pipe flow and in a channel, respectively. In both cases, Lee found that the nonlinear stability criterion is strongly sensitive to the amount of heat transfer, contrary to the linear results by Hsieh [2]. Moreover, Lee's results show that in the nonlinear case the region of stability is bounded above and below, unlike the linear case, which depicts a single neutral curve. All these investigations assumed that the flow is irrotational and the fluid inviscid (IPF, inviscid potential flow).

Recently, Asthana and Agrawal [6] carried out the potential flow analysis of the Kelvin-Helmholtz instability with heat and mass transfer for two viscous fluids confined between two parallel planes. They presented a stability criterion given by a critical relative velocity. They also found that heat and mass transfer has a stabilizing effect when the lower fluid is highly viscous, whereas it has a destabilizing effect when the lower fluid has a low viscosity. Their work is an extension to include heat and mass transfer phenomena of the study of Kelvin-Helmholtz instability of two viscous fluids by Funada and Joseph [7].

In this paper, we investigate the capillary instability problem of a vapor-liquid system in an annular configuration with heat and mass transfer using viscous potential flow (VPF) for axisymmetric disturbances. We follow Hsieh's [2] analysis, assume irrotational motion but, unlike Hsieh, we do not set the fluid viscosity to zero. Therefore, the viscous part of the normal stress enters the analysis; however, the non-slip condition at the boundary is not enforced for irrotational flow. As in Hsieh [2], we assume that the phase change is induced by an interfacial condition for energy transfer which balances the latent heat against conductive heat transfer (see (2.8)), thereby neglecting convection. An antecedent of this work is the study by Funada and Joseph [8], who carried out the viscous potential flow analysis

*Dept. of Aerospace Engineering, KAIST
†Electronic address: trumpet@kaist.ac.kr

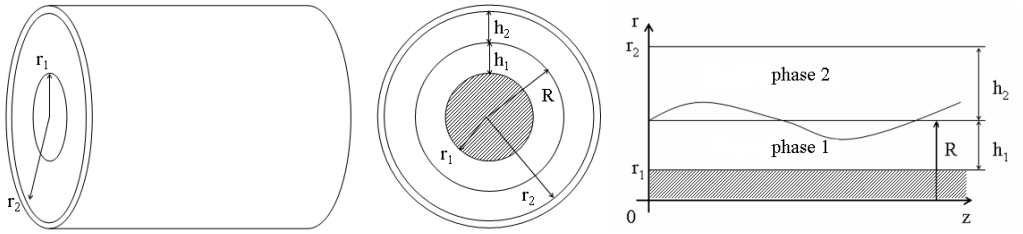

FIG. 1: Schematic of stability analysis

of capillary instability of a cylindrical core of fluid surrounded by another fluid with no heat and mass transfer. They found the condition, in terms of a dimensionless number based on the relevant parameters of the system, for which the growth rate from viscous potential flow closely approaches the solution of the linearized Navier-Stokes equations. Their results show that viscous potential flow is a better approximation of the exact solution than the inviscid model. This motivates the assumption of viscous irrotational motion to carry out the present stability analysis involving phase change and heat transfer. A comprehensive discussion of the theory of viscous potential flow, with numerous examples, can be found in the recent book by Joseph, Funada and Wang [9].

II. PROBLEM FORMULATION

We consider two fluids separated by a cylindrical interface in an annular configuration as in Fig. 1. Both phases 1 and 2 are considered incompressible and irrotational. In the equilibrium state, the inner fluid region $r_1 < r < R$ has thickness h_1, density ρ_1 and viscosity μ_1 and the outer fluid region $R < r < r_2$ has thickness h_2, density ρ_2 and viscosity μ_2. The boundary surfaces at $r = r_1$ and $r = r_2$ are considered to be rigid. The temperatures at $r = r_1$, $r = R$ and $r = r_2$ are T_1, T_0 and T_2, respectively. In the basic state, thermodynamics equilibrium is assumed and the interface temperature T_0 is set equal to the saturation temperature.

Small axisymmetric disturbances are superimposed to the basic state of rest. In the disturbed state, the interface is thus given by

$$F(r, z, t) = r - R - \eta(z, t) = 0, \tag{2.1}$$

where η is the perturbation in the radius of the interface from its equilibrium value. The velocity is expressed as the gradient of a potential and the potential functions satisfy Laplace's equation as a consequence of the incompressibility constraint. That is,

$$\nabla^2 \phi_i = 0. \ (i = 1, 2) \tag{2.2}$$

These potentials are periodic in z.

We assume that phase-change takes place locally in such a way that the net phase-change rate at the interface is equal to zero. The interfacial condition, which expresses the conservation of mass across the interface, is given by

$$\left[\!\left[\rho_i \left(\frac{\partial F}{\partial t} + \nabla \phi_i \cdot \nabla F \right) \right]\!\right] = 0, \tag{2.3}$$

where $[\![x]\!] = x_{R^+} - x_{R^-}$ represents the difference in a quantity as we cross the interface. Then, by used of (2.1), (2.3) becomes,

$$\left[\!\left[\rho_i \left(\frac{\partial \phi_i}{\partial r} - \frac{\partial \eta}{\partial t} - \frac{\partial \eta}{\partial z} \frac{\partial \phi_i}{\partial z} \right) \right]\!\right] = 0 \ \text{ at } r = R + \eta. \tag{2.4}$$

With mass transfer across the interface, the normal stress balance becomes, at $r = R + \eta$,

$$\begin{aligned} \rho_1 (\nabla \phi_1 \cdot \nabla F) \left(\frac{\partial F}{\partial t} + \nabla \phi_1 \cdot \nabla F \right) =& \rho_2 (\nabla \phi_2 \cdot \nabla F) \left(\frac{\partial F}{\partial t} + \nabla \phi_2 \cdot \nabla F \right) \\ &+ (p_2 - p_1 - 2\mu_2 \boldsymbol{n} \cdot \nabla \otimes \nabla \phi_2 \cdot \boldsymbol{n} + 2\mu_1 \boldsymbol{n} \cdot \nabla \otimes \nabla \phi_1 \cdot \boldsymbol{n} + \sigma \nabla \cdot \boldsymbol{n}) \left| \nabla F \right|^2, \end{aligned} \tag{2.5}$$

where p is the pressure, σ is the surface tension coefficient, and $\boldsymbol{n}$ is the normal vector at the interface, respectively. Surface tension has been assumed to be a constant, neglecting its dependence upon temperature, and thereby ignoring any Marangoni effect.

The pressure in (2.5) may be obtained from Bernoulli's equation. When this is done, (2.5) becomes, at $r = R + \eta$,

$$\left[\!\left[\rho_i \left\{ \frac{\partial \phi_i}{\partial t} + \frac{1}{2}\left(\frac{\partial \phi_i}{\partial r}\right)^2 + \left(\frac{1}{2}\frac{\partial \phi_i}{\partial z}\right)^2 - \left[1 + \left(\frac{\partial \eta}{\partial z}\right)^2\right]^{-1} \left(\frac{\partial \phi_i}{\partial r} - \frac{\partial \eta}{\partial z}\frac{\partial \phi_i}{\partial z}\right) \right.\right.$$
$$\left.\left. \times \left(\frac{\partial \phi_i}{\partial r} - \frac{\partial \eta}{\partial t} - \frac{\partial \eta}{\partial t}\frac{\partial \phi_i}{\partial z}\right)\right\} + 2\mu_i \left[\frac{\partial^2 \phi_i}{\partial r^2} - 2\frac{\partial \eta}{\partial z}\frac{\partial^2 \phi_i}{\partial r \partial z} + \frac{\partial^2 \phi_i}{\partial z^2}\left(\frac{\partial \eta}{\partial z}\right)^2\right] \right]\!\right] = \sigma \nabla \cdot \boldsymbol{n}, \tag{2.6}$$

using (2.1). At the wall the normal velocity vanishes, hence,

$$\begin{aligned} \frac{\partial \phi_1}{\partial r} &= 0 \text{ at } r = r_1, \\ \frac{\partial \phi_2}{\partial r} &= 0 \text{ at } r = r_2. \end{aligned} \tag{2.7}$$

The perturbed heat flux at the interface $r = R + \eta(z, t)$ induces phase change. The interfacial condition for this energy transfer proposed by Hsieh [2] is expressed as

$$L\rho_1 \left(\frac{\partial F}{\partial t} + \nabla \phi_1 \cdot \nabla F\right) = S(\eta) \quad \text{at } r = R + \eta, \tag{2.8}$$

where L is the latent heat released from the fluid when is transformed from phase 1 to phase 2 and $S(\eta)$ denotes the net heat flux from the interface. Hsieh [2] indicates that:

> "The expression $S(\eta)$ essentially represents the net heat flux from the interface when such a phase transformation is taking place. In general, the heat fluxes have to be determined from equations governing the heat transfer in the fluids, thus completely coupling the dynamics and the thermal exchanges in the entire flow region. In this simplified version, ... S is simply a function of η, and moreover, S is to be determined from the heat exchange relations in the equilibrium state."

In the equilibrium state, the heat fluxes in the positive r-direction in the fluid phases 1 and 2 are expressed as $-K_1 (T_1 - T_0)/R \ln(r_1/R)$ and $-K_2 (T_0 - T_2)/R \ln(R/r_2)$, respectively where K_1 and K_2 are the heat conductivities of the two fluids. After Hsieh[2], Nayak and Chakraborty [3] wrote this expression for the cylindrical geometry,

$$S(\eta) = \frac{K_2 (T_0 - T_2)}{(R + \eta)[\ln r_2 - \ln(R + \eta)]} - \frac{K_1 (T_1 - T_0)}{(R + \eta)[\ln(R + \eta) - \ln r_1]}, \tag{2.9}$$

and expand it in a Taylor series about $r = R$ as

$$S(\eta) = S(0) + \eta S'(0) + \frac{1}{2}\eta^2 S''(0) + \cdots. \tag{2.10}$$

Then, we take $S(0) = 0$, so that

$$\begin{aligned} G &= \frac{K_2 (T_0 - T_2)}{R \ln(r_2/R)} = \frac{K_1 (T_1 - T_0)}{R \ln(R/r_1)} \\ &= \frac{(T_1 - T_2)/R}{\ln(R/r_1)/K_1 + \ln(r_2/R)/K_2}, \end{aligned} \tag{2.11}$$

indicating that in the equilibrium state the heat fluxes are equal across the vapor-liquid interface. Although the problem has been defined in a somewhat general framework, one can picture the situation of a boiling liquid layer in contact with one of the boundary surfaces and its vapor, considered incompressible, in contact with the other surface. Then, one may apply the model detailed here to the vapor-liquid interface.

III. SOLUTION OF THE LINEARIZED PROBLEM

Linearization of the relations (2.4), (2.6) and (2.8) yields

$$\left[\!\left[\rho_i \left(\frac{\partial \phi_i}{\partial r} - \frac{\partial \eta}{\partial t}\right)\right]\!\right] = 0, \tag{3.1}$$

$$\left[\!\left[\rho_i \frac{\partial \phi_i}{\partial t} + 2\mu_i \frac{\partial^2 \phi_i}{\partial r^2}\right]\!\right] = -\sigma \left(\frac{\partial^2 \eta}{\partial z^2} + \frac{\eta}{R^2}\right), \tag{3.2}$$

$$\rho_1 \left(\frac{\partial \phi_1}{\partial r} - \frac{\partial \eta}{\partial t}\right) = \alpha \eta, \tag{3.3}$$

at $r = R$, where (2.9)-(2.11) have been used to obtain (3.3) and

$$\alpha = \frac{G}{LR} \frac{\ln(r_2/r_1)}{\ln(R/r_1)\ln(r_2/R)}. \tag{3.4}$$

Additionally, Hsieh [2] notes that the "... vapor phase is usually hotter than the liquid phase; therefore α is always positive."

According to (2.2), in cylindrical coordinates, we can write for the harmonic potential $\phi_i(r, z)$, $(i = 1, 2)$,

$$\nabla^2 \phi_i = \frac{\partial^2 \phi_i}{\partial r^2} + \frac{1}{r}\frac{\partial \phi_i}{\partial r} + \frac{\partial^2 \phi_i}{\partial z^2} = 0, \tag{3.5}$$

with boundary conditions (2.7) at the wall.

We use standard normal mode decomposition to find solutions of the above set of governing equations. Let

$$\eta = C \exp(\mathrm{i}kz - \mathrm{i}\omega t) + \text{c.c.} = CE + \text{c.c.}, \tag{3.6}$$

where C is constant, $E \equiv \exp(\mathrm{i}kz - \mathrm{i}\omega t)$, i is the imaginary unit, k is the real wavenumber, $\omega = \omega_R + \mathrm{i}\omega_I$ is the complex frequency and c.c. represents the complex conjugate of the previous term. Hence, solutions for the velocity potential have the form,

$$\begin{aligned} \phi_1 &= \frac{1}{k}\left(\frac{\alpha}{\rho_1} - \mathrm{i}\omega\right) A_0(k, r) CE + \text{c.c.}, \\ \phi_2 &= \frac{1}{k}\left(\frac{\alpha}{\rho_2} - \mathrm{i}\omega\right) B_0(k, r) CE + \text{c.c.}, \end{aligned} \tag{3.7}$$

where

$$\begin{aligned} A_0(k, r) &= \frac{I_0(kr)K_1(kr_1) + I_1(kr_1)K_0(kr)}{I_1(kR)K_1(kr_1) - I_1(kr_1)K_1(kR)}, \\ B_0(k, r) &= \frac{I_0(kr)K_1(kr_2) + I_1(kr_2)K_0(kr)}{I_1(kR)K_1(kr_2) - I_1(kr_2)K_1(kR)}, \end{aligned}$$

and I_n, K_n are modified Bessel functions of the first and second kind. In writing (3.7), constraints (3.1) and (3.2) have been satisfied.

IV. DISPERSION RELATION

A. Dimensional form

Substituting (3.6) and (3.7) into (3.2), we find

$$D(\omega, k) = a_0\omega^2 + \mathrm{i}a_1\omega + a_2 = 0, \tag{4.1}$$

where

$$\begin{aligned} a_0 =& \rho_1 A_0(k, R) - \rho_2 B_0(k, R), \\ a_1 =& \alpha\left[A_0(k, R) - B_0(k, R)\right] + 2k^2\left[\mu_1 A_t(k, R) - \mu_2 B_t(k, R)\right], \\ a_2 =& -\sigma k\left(k^2 - \frac{1}{R^2}\right) - 2\alpha k^2\left[\frac{\mu_1}{\rho_1} A_t(k, R) - \frac{\mu_2}{\rho_2} B_t(k, R)\right], \end{aligned}$$

$$A_t(k,R) = A_{0,rr}(k,R) = A_0(k,R) - \frac{1}{kR},$$
$$B_t(k,R) = B_{0,rr}(k,R) = B_0(k,R) - \frac{1}{kR},$$

where the subscript 'rr' denotes a second partial derivative with respect to r. For $\omega = \omega_R + \mathrm{i}\omega_I$, the quadratic equation (4.1) is separated into the real and imaginary parts. After eliminating ω_R, we obtain the following expression for the growth rate ω_I:

$$a_0\omega_I^2 + a_1\omega_I - a_2 = 0. \tag{4.2}$$

Neutral curves, $\omega_I(k) = 0$, are generated by the condition $a_2 = 0$, which implies,

$$\sigma\left(k_c^2 - \frac{1}{R^2}\right) + 2\alpha k_c\left[\frac{\mu_1}{\rho_1}A_t(k_c,R) - \frac{\mu_2}{\rho_2}B_t(k_c,R)\right] = 0, \tag{4.3}$$

where k_c denotes the critical wavenumber. Expression (4.3) reveals that the effects of heat and mass transfer carried by α enters into the definition of the neutral curve if the viscous effects of the irrotational motion are considered in the analysis. For inviscid potential flow (see also Lee[4]), the critical wavenumber $k_c = 1/R$ is independent of α. For zero heat flux ($\alpha = 0$), both VPF and IPF predicts the same k_c.

B. Dimensionless form

To write the dispersion relation in dimensionless form we introduce the following dimensionless groups,

$$\hat{r} = r/H,\ \hat{z} = z/H,\ \hat{\eta} = \eta/H,$$
$$\hat{t} = t/\tau,\ \hat{\omega} = \omega\tau,\ \hat{k} = kH,$$
$$\varphi = \frac{h_1}{H},\ \hat{R} = \hat{r}_1 + \varphi,$$

where the length scale H and the time scale τ are defined as

$$H = h_1 + h_2 = r_2 - r_1,$$
$$\tau = \sqrt{\frac{\rho_2 H^3}{\sigma}},$$

and φ denotes the dimensionless vapor thickness. Furthermore,

$$\ell = \frac{\rho_1}{\rho_2},\ m = \frac{\mu_1}{\mu_2},$$
$$\kappa = \frac{\nu_1}{\nu_2} = \frac{m}{\ell} \ \text{ with } \ \nu_1 = \frac{\mu_1}{\rho_1},\ \nu_2 = \frac{\mu_2}{\rho_2},$$

and

$$Oh = \frac{\sqrt{\rho_2\sigma H}}{\mu_2},\ \hat{\alpha} = \frac{\alpha}{\rho_2/\tau},$$

where Oh is the Ohnesorge number and we denote $\hat{\alpha}$ as the heat-transfer capillary group. Notice that surface tension, which is essential in the description of the phenomena, is contained in these two dimensionless groups.

Eliminating the '$\hat{}$' on the dimensionless variables for brevity, (4.1) may be written in dimensionless form as

$$D(\omega,k) = a_0\omega^2 + \mathrm{i}a_1\omega + a_2 = 0, \tag{4.4}$$

where

$$a_0 = \ell A_0(k,R) - B_0(k,R),$$

$$a_1 = \alpha \left[A_0(k,R) - B_0(k,R)\right] + \frac{2}{Oh}k^2 \left[mA_t(k,R) - B_t(k,R)\right],$$
$$a_2 = -k\left(k^2 - \frac{1}{R^2}\right) - \frac{2\alpha}{Oh}k^2\left[\frac{m}{\ell}A_t(k,R) - B_t(k,R)\right].$$

From (4.3), the expression for the neutral curve becomes

$$\left(k_c^2 - \frac{1}{R^2}\right) + \Lambda k_c \left[\kappa A_t(k_c,R) - B_t(k_c,R)\right] = 0, \tag{4.5}$$

with an alternative heat-transfer capillary dimensionless group

$$\Lambda = \frac{2\alpha}{Oh}, \tag{4.6}$$

which is introduced for convenience.

From (4.5), we can define $f(k)$ for fixed R as

$$f(k) \equiv \left(k^2 - \frac{1}{R^2}\right) + \Lambda k \left[\kappa A_t(k,R) - B_t(k,R)\right]. \tag{4.7}$$

From (4.7), we find that $f(k) = f(-k)$, $f(0)$ is a minimum and $f(k)$ is concave. Thus $f(0) < 0$ is a necessary condition for which k_c ($k_c > 0$) exists. When a real $k_c > 0$ cannot be obtained, the fluid configuration is stable.

For $k \sim 0$, the asymptotic form of $f(k)$ is

$$\left(k^2R^2 - 1\right) + \Lambda R^2\left[\kappa\left(\frac{2R}{R^2 - r_1^2} - \frac{1}{R}\right) + \frac{2R}{r_2^2 - R^2} + \frac{1}{R}\right] = 0. \tag{4.8}$$

Then, there is no critical wavenumber $k_c > 0$ under the following condition for which $f(0) > 0$:

$$\Lambda R^2\left[\kappa\left(\frac{2R}{R^2 - r_1^2} - \frac{1}{R}\right) + \left(\frac{2R}{r_2^2 - R^2} + \frac{1}{R}\right)\right] > 1, \tag{4.9}$$

or

$$\Lambda R^2\left[\kappa\left(\frac{R^2 + r_1^2}{R^2 - r_1^2}\right) + \frac{R^2 + r_2^2}{r_2^2 - R^2}\right] > 1. \tag{4.10}$$

V. COMPUTATION AND DISCUSSION OF RESULTS - VISCOUS STABILIZATION OF WATER-STEAM SYSTEMS

In this section we carry out computations using the expressions presented in the previous sections for a film boiling condition. We take water and steam as working fluids. Referring to Fig. 1, the steam and water are identified with phase 1 and phase 2, respectively, such that $T_1 > T_0 > T_2$. In film boiling, the water-steam interface is in saturation condition and the temperature T_0 is set equal to the saturation temperature. The properties of both phases are determined for this condition. The diameter of the inner and outer cylinder are 1 and 2 mm, respectively. By knowing the vapor thickness and two temperatures of the triad (T_0, T_1, T_2), the heat flux and the unknown temperature can be predicted from the conduction model (2.11).

The results from the viscous potential flow analysis of capillary instability with heat and mass transfer are presented in Fig. 2 for the growth rate ω_I versus the wavenumber k from (4.4). In this numerical experiment, the temperature of interface T_0 is set to $400K$. The entire shape of the growth rate graph is similar to the inviscid case but with heat and mass transfer having stabilizing effects in the irrotational flow of viscous fluids. Comparing results from IPF with those from VPF in Fig. 2(a) and 2(b), we notice that the interval of wavenumbers for unstable waves shrinks with increasing α according to VPF. However, for a dimensionless vapor thickness of $\varphi = 0.10$ the stabilizing effect of viscosity is negligible as shown in Fig. 2(c) and 2(d). This is analyzed later in this section. As we shall see, there is a threshold α for which VPF renders all waves stable. In contrast, IPF results show that, by neglecting the viscous effects of the irrotational flow, the maximum length (or minimum wavenumber) of stable waves becomes insensitive to heat and mass transfer phenomena. Hence, the system is always unstable according to IPF as shown by Lee [4]. In addition, comparing Fig. 2(a) and Fig. 2(c) for IPF and $\varphi = 0.01$ and $\varphi = 0.1$, respectively, we notice that the maximum growth rate ω_{Im} decreases the fastest with the parameter α for the smallest vapor thickness. Similar trend

is observed for VPF from Fig. 2(b) and Fig. 2(d). VPF graphs also reveal that viscosity damps the maximum growth rate with respect to the IPF value for the same α.

Table I compares the maximum growth rate ω_{Im}, related wavenumber k_m and critical wavenumber k_c as function of the heat-transfer capillary number α (dimensionless) for IPF and VPF. The difference between the α scales are due to the change of dimensionless vapor thickness φ, from 0.01 to 0.1. This table confirms that the maximum growth rate for IPF and VPF decreases with α, with ω_{Im} from VPF decreasing with the fastest rate. Also, VPF renders lower values of ω_{Im} than IPF for the same α. By comparing results for $\varphi = 0.01$ and $\varphi = 0.1$, we notice that discrepancies between IPF and VPF substantially diminish as the vapor fraction increases. In this table, the last lines of results for $\varphi = 0.01$ and $\varphi = 0.1$ show the critical α for which $k_c = 0$ according to VPF, corresponding to a stable interface. Notice that the threshold α for the higher vapor thickness $\varphi = 0.1$ is larger than the critical α associated with the lower $\varphi = 0.01$

Graphs of the critical wavenumber k_c versus the kinematic viscosity ratio κ are presented for various Λ values and $\varphi = 0.01$ in Fig. 3 according to (4.5). In contrast with Fig. 2, this figure is not exclusive for the water-steam system. We observe that for every Λ there exists a critical κ for which all waves are stable. This critical value decreases as the heat-transfer capillary number Λ increases. For unstable waves ($k_c > 0$), increasing κ for fixed Λ decreases the size of the interval of wavenumbers for unstable waves. k_c from VPF is bounded above by the inviscid result for all Λ.

Fig. 4(a) shows the critical wavenumber k_c as function of the dimensionless vapor thickness φ and heat-transfer capillary number Λ according to VPF from (4.5) for $\kappa = 41.3218$ (water-steam at $T_0 = 400K$). Comparing with the case $\Lambda = 0$ where no heat and mass transfer occurs, $k_c = 1/R$, which in turn is equivalent to the inviscid result, the critical wavenumber is the most sensitive to heat and mass transfer effects for lower vapor thickness φ. In particular, for the highest Λ considered in the analysis ($= 10 \times 10^{-4}$), the system is stable. For this Λ, the discrepancy with the $\Lambda = 0$ case is noticeable for the entire φ interval. The trend indicates that increasing Λ for fixed φ reduces the interval of unstable waves, which can be completely suppressed. By contrast, the graphs for the lower nonzero Λ ($= 0.1 \times 10^{-4}$ and 10×10^{-4}) reach the inviscid result for $\varphi > 0.2$, nearly. This result follow the tendency shown in Table I for $\varphi = 0.1$. Figure 4(b) shows graphs of k_c versus φ for two values of Λ and κ. Notice that while keeping Λ constant, increasing κ reduces k_c for fixed φ; hence, longer stable waves are predicted by the model. As a side note regarding Fig. 4, we observe in (3.4) and (4.6) that Λ is a function of the dimensionless vapor thickness φ, through R. Keeping Λ fixed while changing φ implies that other parameters must change, for instance, the heat flux. It is also evident from Fig. 4 that the graphs for $\Lambda = 1.0 \times 10^{-4}$ and $\Lambda = 10.0 \times 10^{-4}$ depict a maximum k_c associated with certain thickness φ; this thickness increases when Λ increases for fixed κ and when κ decreases for fixed Λ.

Our results thus show that linear analysis of capillary instability with heat and mass transfer predicts a region of stability unbounded above ($k_c \leq k < \infty$) for viscous and inviscid potential flow, so that short waves are stable. In contrast, as shown by Lee [4], nonlinear inviscid analysis surprisingly predicts a region of stability with upper and lower bounds, thereby leading to both long and short unstable waves. Similar to our trends (see Fig. 2 and Table I), Lee's nonlinear analysis predicts that the width of the band of stability decreases by increasing the vapor thickness, and becomes wider by increasing the heat flux.

Two competing mechanisms play major roles in the dynamics of the perturbed interface. On one side, the capillary forces promotes the instability of the cylindrical interface, while, on the other side, heat and mass transfer effects help to stabilize the interface. In the frame of Hsieh's purely heat-conduction model, the latter mechanism is explained in terms of local evaporation and condensation at the interface. At a perturbed interface, crests are warmer because they are closer to the hotter boundary on the vapor side, thus local evaporation occurs, whereas troughs are cooler and thus condensation takes place. A comprehensive discussion of phase-change effects in interfacial stability is presented by Ozen and Narayanan [10], who considered not only heat conduction but also convection. However, their system consisted of a liquid underlying its vapor between two parallel plates, where the plate in the liquid side is hotter. In this setup, the evaporation-condensation phenomena promotes instability, which is mitigated by surface tension for short waves, in opposition to the physics described above for the system investigated in the present work.

The destabilizing effects of surface tension and the stabilizing effects of heat transfer are demonstrated in the model of the critical wavenumber k_c given in (4.5) through the dimensionless group Λ defined in (4.6). Indeed, one can readily show that Λ is directly proportional to the heat flux and inversely proportional to surface tension. Therefore, when surface tension increases, the wavenumber interval for unstable waves becomes wider as Λ decreases for fixed κ (see Fig. 3).

Concerning convective heat transfer, its effects on the dynamics of the liquid-vapor interface may be significant [10, 11]. Certainly, the transport of heat by the motion of warmer or cooler fluid elements between crests and troughs in either side of the interface can influence the stability features of heat conduction described above. However, to simplify the analysis, Hsieh's assumption of modeling heat conduction disregarding convection has been adopted to elucidate the role in capillary instability of the interaction of heat and mass transfer with the viscous effects of the irrotational motion. Including convection in the viscous potential flow analysis of capillary instability with heat transfer and phase change will lead to more compelling results and is a matter for future work.

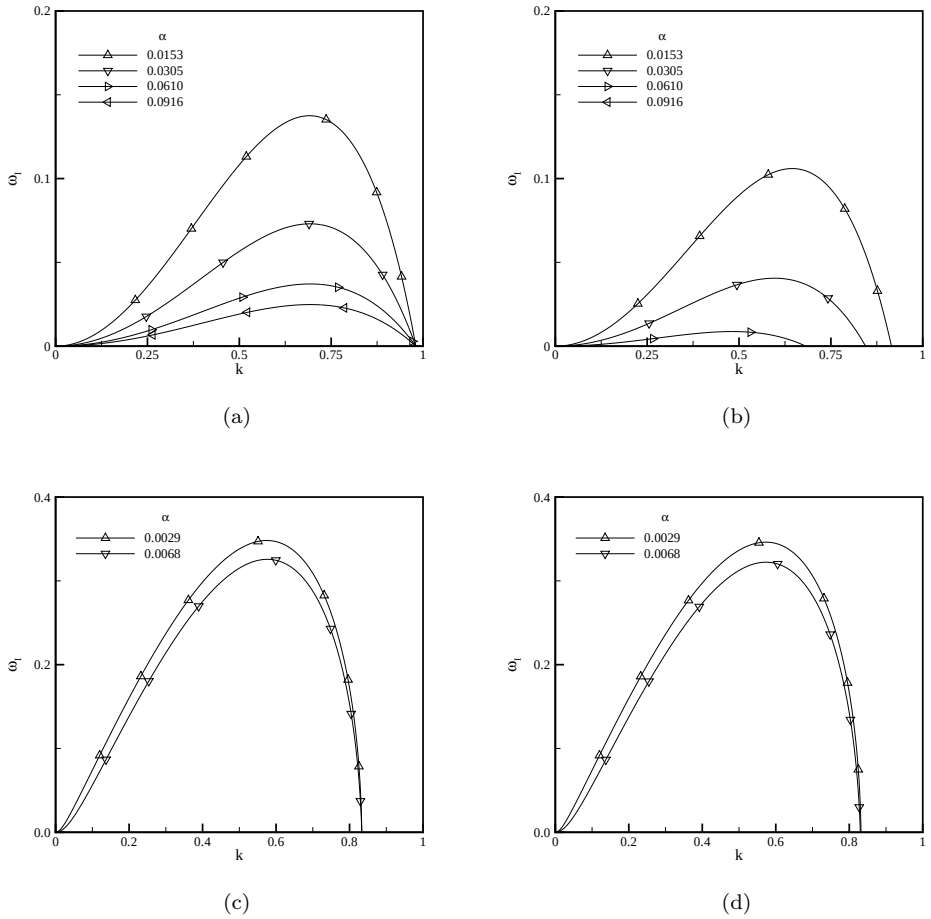

FIG. 2: Growth rate ω_I versus wavenumber k for a series of heat-transfer-capillary number α values according to (4.4) for the water-steam system; (a) φ=0.01, IPF (b) φ=0.01, VPF, (c) φ=0.1, IPF (d) φ=0.1, VPF. In these computations $\ell = 0.0015$, $m = 0.0604$ and $Oh = 1012$ obtained for $T_0 = 400K$.

A final remark on the assumption of irrotational motion is due. This approximation implies that the flow field does not satisfy the non-slip condition at the bounding surfaces and, consequently, the boundary layers at these locations are ignored. Similarly, vorticity layers on both sides of the interface are also disregarded and continuity of tangential velocity and stress at this position is not enforced. In making this assumption, we are encouraged by the results obtained by Funada and Joseph [8]. Using viscous potential flow as an approximation of the linearized Navier-Stokes analysis of capillary instability of a fluid cylinder in another fluid with no heat and mass transfer, they carried computations with more than a dozen of fluid pairs and concluded that VPF approximates the exact solution for gas-liquid or liquid-liquid flows when a dimensionless surface tension Oh^2 is greater than $O(10)$, where Oh is determined with the properties of the most viscous fluid; otherwise, potential flow is off the mark and internal vorticity generation significantly affects the dynamics of the interface. In the frame of the problem discussed here, boundary-layer flow impacts the interface stability through the diffusion of momentum and the transport of heat by convection in either side of the interface.

VI. CONCLUSION

In this paper, we studied the capillary instability to linear perturbations of the cylindrical interface of two incompressible fluids confined in a concentric annulus with heat and mass transfer using viscous potential flow. Heat transfer is modeled exclusively as a conduction process. We obtained the dispersion relation describing the stability of the system in terms of various dimensionless numbers, namely, density and viscosity ratios, dimensionless inner radius and phase fraction, Ohnesorge number and a phase change parameter depending upon the geometry, the temperature

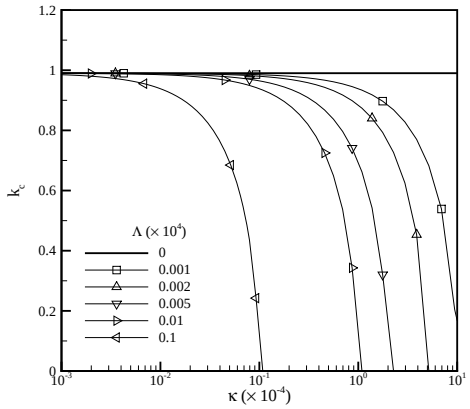

FIG. 3: Critical wavenumber k_c versus kinematic viscosity ratio κ for a series of heat-transfer-capillary group Λ values and dimensionless vapor thickness φ =0.01 according to (4.5). For every Λ, there is a critical κ above which all waves are stable.

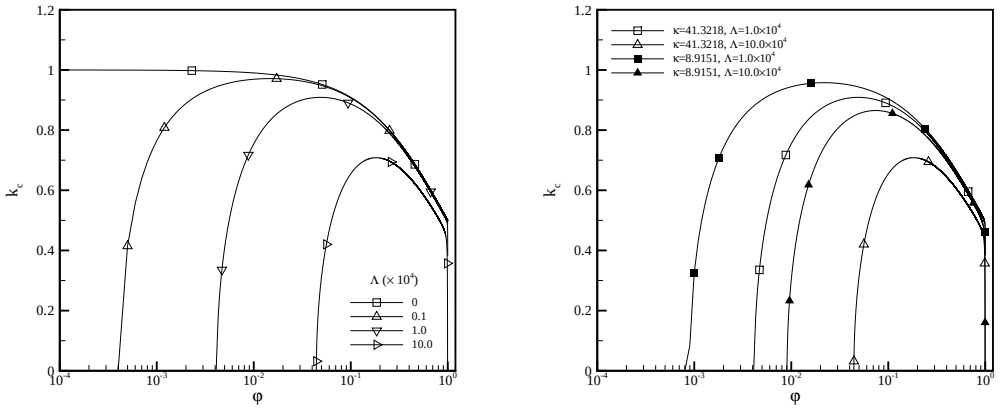

(a) (b)

FIG. 4: Critical wavenumber k_c versus dimensionless vapor thickness φ for different values of the heat-transfer-capillary number Λ according to (4.5) for the water-steam system: (a) for $\kappa = 41.3218$, $\ell = 0.0015$ and $Oh = 1012$ obtained for $T_0 = 400K$, (b) Comparison with graphs for $\kappa = 8.9151$, $\ell = 0.0159$ and $Oh = 1378$ obtained for $T_0 = 500K$. The effects of heat and viscosity become outstanding for low vapor thickness.

difference, and fluid properties including latent heat. We applied the model to the film-boiling condition in which the liquid is in contact with the cooler outer boundary and its own vapor is in contact with the warmer inner boundary. Our main result is that, for the irrotational motion of two viscous fluids, heat and mass transfer phenomena can completely stabilize the interface against capillary effects. This conclusion cannot be achieved for inviscid fluids. Moreover, we found that the viscous effects of the irrotational motion interacting with heat and mass transfer reduce the maximum growth rate and increase the length of the wave with the maximum growth rate, in comparison with the inviscid case. As the vapor thickness increases, the difference between inviscid and viscous potential flow becomes less conspicuous.

TABLE I: Maximum growth rate parameters and critical wavenumber as function of the heat-transfer-capillary number α and dimensionless vapor thickness φ according to (4.4) for the water-steam system ($\ell = 0.0015$, $m = 0.0604$ and $Oh = 1012$ obtained for $T_0 = 400K$).

φ=0.01						
		IPF			VPF	
α	ω_{Im}	k_m	k_c	ω_{Im}	k_m	k_c
0.0000	0.4891	0.6672	0.9804	0.4855	0.6646	0.9804
0.0153	0.1375	0.6910	0.9804	0.1060	0.6448	0.9150
0.0305	0.0730	0.6924	0.9804	0.0406	0.5964	0.8446
0.0458	0.0493	0.6928	0.9804	0.0186	0.5424	0.7676
0.0610	0.0371	0.6928	0.9804	0.0087	0.4820	0.6820
0.0763	0.0298	0.6930	0.9804	0.0038	0.4128	0.5840
0.0916	0.0248	0.6930	0.9804	0.0000	0.0002	0.0002
0.1206	0.0189	0.6930	0.9804	0.0000	0.0000	0.0000
φ=0.10						
		IPF			VPF	
α	ω_{Im}	k_m	k_c	ω_{Im}	k_m	k_c
0.0000	0.3661	0.5732	0.8334	0.3652	0.5724	0.8334
0.0010	0.3600	0.5736	0.8334	0.3588	0.5726	0.8330
0.0019	0.3540	0.5742	0.8334	0.3524	0.5728	0.8326
0.0029	0.3482	0.5746	0.8334	0.3462	0.5730	0.8320
0.0039	0.3424	0.5750	0.8334	0.3401	0.5732	0.8316
0.0048	0.3367	0.5754	0.8334	0.3340	0.5734	0.8312
0.0058	0.3312	0.5758	0.8334	0.3281	0.5734	0.8306
0.0068	0.3257	0.5762	0.8334	0.3223	0.5736	0.8302
12.143	0.0009	0.5878	0.8334	0.0000	0.0000	0.0000

Acknowledgments

H. Kim wishes to thank Daniel D. Joseph for his encouragement and engaging discussions of matters related to this research.

[1] D. Y. Hsieh, "Effects of heat and mass transfer on rayleigh-taylor instability", Trans. ASME, J. Basic, Eng., Vol. 94D, pp. 156-162, 1972.
[2] D. Y. Hsieh, "Interfacial stability with mass and heat transfer", Phys. Fluds, Vol. 21, pp. 745-748, 1978.
[3] A. R. Nayak and B. B. Chakraborty, "Kelvin-Helmholtz stability with mass and heat transfer", Phys. Fluids, Vol. 27, pp. 1937-1941, 1984.
[4] D. S. Lee, "Nonlinear Rayleigh instability of cylindrical flow with mass and heat transfer", J. Phys. A : Math. Gen., Vol. 36, pp. 573-583, 2003.
[5] D. S. Lee, "Nonlinear Kelvin-Helmholtz instability of fluid layers with mass and heat transfer", J. Phys. A : Math. Gen., Vol. 38, pp. 2803-2817, 2005.
[6] R. Asthana and G. S. Agrawal, "Viscous potential flow analysis of Kelvin-Helmholtz instability with mass transfer and vaporization", Physica A : Stat. Mech. Appl., Vol. 382, pp. 389-404, 2007.
[7] T. Funada and D. D. Joseph, "Viscous potential flow analysis of Kelvin-Helmholtz instability in a channel", J. Fluid Mech., Vol. 445, pp. 263-283, 2001.
[8] T. Funada and D. D. Joseph, "Viscous potential flow analysis of capillary instability", Int. J. Multiphase Flow, Vol. 28, pp. 1459-1478, 2002.
[9] D. D. Joseph and T. Funada and J. Wang, *Potential flows of viscous and viscoelastic fluids*, Cambridge University Press., NY, 2007.
[10] O. Ozen and R. Narayanan, "The physics of evaporative and convective instabilities in bilayer systems: Linear theory", Phys. Fluids, Vol. 16, pp. 4644-4652, 2004.
[11] O. Ozen and R. Narayanan, "The physics of evaporative instabilities in bilayer systems: Weak non-linear theory", Phys. Fluids, Vol. 16, pp. 4653-4660, 2004.